ARTHRITIS & RHEUMATISM
Vol. 60, No. 8, August 2009, pp 2513–2523
DOI 10.1002/art.24682

Amelioration of Alphavirus-Induced Arthritis and Myositis in a Mouse Model by Treatment With Bindarit, an Inhibitor of Monocyte Chemotactic Proteins

Nestor E. Rulli,[1] Angelo Guglielmotti,[2] Giorgina Mangano,[2] Michael S. Rolph,[1] Claudia Apicella,[2] Ali Zaid,[1] Andreas Suhrbier,[3] and Suresh Mahalingam[1]

Objective. **Alphaviruses such as chikungunya virus, Sindbis virus, o'nyong-nyong virus, Mayaro virus, and Ross River virus (RRV), are commonly associated with arthralgias and overt arthritides worldwide. Understanding the processes by which arthritogenic viruses cause disease is a prerequisite in the quest for better treatments. In this regard, we have recently established that monocyte/macrophages are mediators of alphavirus-induced arthritis in mice. We hypothesized that chemokines associated with monocyte/macrophage recruitment may play an important role in disease. The aim of the present investigations was to determine whether bindarit, an inhibitor of monocyte chemotactic protein (MCP) synthesis, could ameliorate alphavirus-induced rheumatic disease in mice.**

Methods. **Using our recently developed mouse model of RRV-induced arthritis, which has many characteristics of RRV disease (RRVD) in humans, the effects of bindarit treatment on RRVD in mice were determined via histologic analyses, immunohistochemistry, flow cytometry, real-time polymerase chain reaction analysis, enzyme-linked immunosorbent assay, and electrophoretic mobility shift assay.**

Results. **Bindarit-treated RRV-infected mice developed mild disease and had substantially reduced tissue destruction and inflammatory cell recruitment as compared with untreated RRV-infected mice. The virus load in the tissues was not affected by bindarit treatment. Bindarit exhibited its activity by down-regulating MCPs, which in turn led to inhibition of cell infiltration and lower production of NF-κB and tumor necrosis factor α, which are involved in mediating tissue damage.**

Conclusion. **Our data support the use of inhibitors of MCP production in the treatment of arthritogenic alphavirus syndromes and suggest that bindarit may be useful in treating RRVD and other alphavirus-induced arthritides in humans.**

Mosquito-borne arthritogenic alphaviruses, such as the Sindbis group of viruses, the Asian/African chikungunya virus, the African o'nyong-nyong virus, the South American Mayaro virus, and the Australian Barmah Forest virus and Ross River virus (RRV), are frequently associated with outbreaks of polyarthritis and/or polyarthralgia in humans (1). For example, a recent chikungunya virus epidemic in the Indian Ocean resulted in ~250,000 cases on La Réunion Island (2), >3 million cases in India (3), and ~200 cases in Italy (4). Between 1959 and 1962, an epidemic of o'nyong-nyong fever in Africa affected at least 2 million people (5), and RRV caused a large epidemic of RRV disease (RRVD) in 1979–1980, resulting in ~60,000 cases in the South Pacific (6).

RRV is a positive-sense single-stranded alphavirus. It is transmitted by mosquitoes and is endemic in Australia and Papua New Guinea, causing up to 8,000 cases of RRVD annually in Australia in recurrent seasonal epidemics (7). In humans, the dominant symptom of RRVD is arthralgia and/or arthritis, with many patients also experiencing myalgia and fatigue and some experiencing fever and rash (8). Joint symptoms most

Supported by the Australian National Health and Medical Research Council (NHMRC project grants 303404 and 508600).

[1]Nestor E. Rulli, PhD, Michael S. Rolph, PhD, Ali Zaid, PhD, Suresh Mahalingam, PhD: University of Canberra, Canberra, ACT, Australia; [2]Angelo Guglielmotti, PhD, Giorgina Mangano, PhD, Claudia Apicella, BSc: Angelini Research Center, Rome, Italy; [3]Andreas Suhrbier, PhD: Queensland Institute of Medical Research, Brisbane, Australia.

Address correspondence and reprint requests to Suresh Mahalingam, PhD, Faculty of Applied Science, University of Canberra, Canberra, ACT 2601, Australia. E-mail: suresh.mahalingam@canberra.edu.au.

Submitted for publication April 8, 2008; accepted in revised form April 15, 2009.

commonly involve the fingers, knees, and ankles, but many joints can be affected. The disease is often severe and debilitating at onset, and it progressively resolves over 3–6 months in the majority of patients (9,10). Using validated quality-of-life questionnaires, the severity of RRVD at onset was shown to be comparable with that seen in patients with osteoarthritis awaiting hip or knee replacements or in patients with chronic rheumatoid arthritis (RA) or Lyme arthritis (9).

The pathologic and/or immunopathologic mechanisms responsible for viral arthropathies are poorly understood, largely because of the absence of small animal models of disease. Recently, we established a mouse model of RRVD that recapitulates many aspects of RRVD in humans and thus provides one of the first mouse models for the study of viral arthritis (11,12). RRV infection in mice results in inflammation of the joints and skeletal muscles and a disease that is characterized by progressive symmetric hind limb dysfunction, ranging from loss of hind limb gripping ability to very severe hind limb dragging (13).

Macrophages appear to play a central role in mediating the disease in this model (12,13), an observation that is consistent with the presence of numerous monocytes and activated macrophages in the synovial infiltrates of RRVD patients (14). Macrophages and their products are also central players in the pathogenesis of RA (15), with a range of cytokines (16) and chemokines (17) being used, or considered for use, as targets for therapeutic interventions.

The spectrum of the mediators of inflammation that are involved in viral arthritides has been less well studied. Interferon-γ (IFNγ), tumor necrosis factor α (TNFα), and monocyte chemotactic protein 1 (MCP-1; CCL2) have been detected in synovial effusions from RRVD patients, and macrophage-dependent secretion of IFNγ, TNFα, interleukin-1β (IL-1β), and MCP-1 is implicated in the immunopathogenesis of RRVD in the mouse model (12). Furthermore, RRV-infected macrophages and synovial fibroblasts secrete MCP-1 and IL-8 (18).

RRVD and other viral arthritides are usually treated with nonsteroidal antiinflammatory drugs (NSAIDs), which provide only partial relief, and better treatments are clearly needed. We describe herein the effect of bindarit in the mouse model of RRV-induced arthritis and myositis. Bindarit is an indazole derivative representing a novel class of inhibitors capable of reducing chemokine synthesis. The drug exerts potent antiinflammatory activity but does not cause systemic immunosuppression and does not affect arachidonic acid metabolism. Treatment with bindarit ameliorates joint damage in rat adjuvant-induced arthritis (19), limits glomerular injury and prolongs survival of NZB/W lupus mice (20,21), and protects mice against acute pancreatitis (22). Several studies have demonstrated that bindarit is an inhibitor of MCP-1 production in vitro and in vivo and have suggested that its beneficial effects on animal models of inflammation are related to this anti–MCP-1 activity (21–24). More recently, bindarit has also been shown to selectively inhibit the production of MCP-2 and MCP-3 in human monocytes in vitro (25).

Clinical trials have confirmed the positive safety profile of bindarit, and it is orally available, which is an enormous advantage for the treatment of chronic inflammatory conditions (26). In preliminary clinical studies, oral treatment with bindarit was shown to have analgesic activity, to significantly affect pannus density in RA patients, as demonstrated by nuclear magnetic resonance imaging, as well as to mediate a significant reduction in urinary albumin excretion and urinary MCP-1 levels in lupus nephritis patients (26).

In the present study, we found that bindarit treatment ameliorated RRVD symptoms in mice, reduced muscle and joint inflammation, and limited muscle damage. The drug down-regulated the expression of MCPs in vivo and inhibited macrophage recruitment into the joints and muscle tissues. These studies not only provide insights into the immunopathologic mechanisms responsible for RRVD but also suggest that inhibitors of the production of MCPs, such as bindarit, have potential benefit in the treatment of alphaviral arthritides and perhaps other viral arthropathies as well.

MATERIALS AND METHODS

Virus. Stocks of the T48 strain of RRV were produced by transcription of the pRR64 plasmid, which encodes the T48 complementary DNA (cDNA) clone (27). The transcripts were electroporated into Vero cells, and the supernatant was collected and concentrated by centrifugation (model CP90WX; Hitachi, Tokyo, Japan) as described elsewhere (11).

Mice. C57BL/6 (B6) mice were obtained from the Animal Resources Centre (Canning Vale, Western Australia, Australia). The 21-day-old mice were inoculated subcutaneously in the pectoral area with 10^3 plaque-forming units (PFU) of RRV diluted in phosphate buffered saline (PBS; 20-μl volume). Mock-inoculated mice were injected with diluent alone. Mice were weighed and scored for disease symptoms every 24 hours. Signs of disease were determined by assessing grip strength and gait. Disease signs were scored as follows: 0 = no disease, 1 = ruffled fur, 2 = very mild hind limb weakness, 3 = mild hind limb weakness, 4 = moderate hind limb weakness, 5 = severe hind limb weakness/dragging, 6 = complete loss of hind limb function, 7 = moribund, and 8 =

dead. The experiments were approved by the Animal Ethics Committee of the University of Canberra.

Bindarit treatment of mice. Bindarit (2-methyl-2-[[1-(phenylmethyl)-1*H*-indazol-3-yl]methoxy] propanoic acid) was provided by Angelini Research Center/ACRAF (Rome, Italy).

RRV infection studies. Mice inoculated with RRV were injected intraperitoneally (IP) with bindarit (100 mg/kg of body weight in a 100-μl volume) or vehicle (0.5% methylcellulose; Sigma, Castle Hill, New South Wales, Australia) twice a day starting from the day of infection. Mice were weighed and monitored for disease symptoms daily. Disease signs were scored as described above. In a separate experiment, mice were treated with bindarit or vehicle twice a day starting from day 6 after infection. Mice were monitored for disease symptoms as described above.

Lipopolysaccharide (LPS) treatment studies. Mice were injected IP with bindarit or vehicle and, 30 minutes later, were injected IP with LPS (100 μg/mouse; Difco, Detroit, MI). One day after treatment, mice were killed, and blood was collected for serum cytokine analyses.

MCP-1 depletion studies. Neutralization of MCP-1 was performed by IP injection of 200 μg of IgG-purified rabbit anti–MCP-1 or control IgG on days 1, 3, 6, and 8 after infection. Mice were monitored for disease symptoms as described above.

Bindarit treatment of MonoMac cells. MonoMac6, a human macrophage-like cell line, was kindly provided by Prof. A. Mantovani (Istituto Clinico Humanitas, Istituto di Recovero e Cura a Carattere Scientifico, Milan, Italy). Cells were maintained in RPMI 1640 medium supplemented with 10% fetal bovine serum (EuroClone, Wetherby, UK), 2% L-glutamine (EuroClone), 1% penicillin/streptomycin solution, 1% nonessential amino acids, 1 m*M* sodium pyruvate, and 1 n*M* oxaloacetic acid (all from Sigma), at 37°C in a humidified atmosphere consisting of 5% CO_2. Cells (5×10^4/well) were seeded into 96-well plates in 200 μl of medium that had or had not been pretreated for 1 hour with bindarit (300 μM) and were then stimulated with 100 ng/ml of LPS (Sigma) for 4 or 20 hours. Bindarit stock solution was prepared in DMSO (Sigma) and diluted in RPMI 1640 (0.1% final concentration of DMSO). Following incubation, the plate was centrifuged at 3,000*g* for 7 minutes, and the supernatant was removed and stored at –80°C until used to measure cytokine levels. Plates containing cell pellets were stored at –80°C until used to quantify gene expression.

Cell growth and virus assay. Mice were killed, and the quadriceps muscles and ankle joints were removed for determination of virus titers by plaque assay on Vero cells, as previously described (11).

Histologic analysis. Mice used for histologic analyses were killed and perfused with buffered formalin. Muscle and joint tissues were fixed in formalin for 24 hours and 72 hours, respectively. Paraffin-embedded, hematoxylin and eosin (H&E)–stained sections were prepared by the Histology Unit of the Australian National University (Canberra, ACT, Australia). H&E-stained slides were analyzed using a Leica CME microscope (Leica Microsystems, Wetzlar, Germany). For cryosections, tissues were embedded in OCT compound (Tissue-Tek; Miles, Elkhart, IN) immediately after harvesting and were frozen in a dry ice/acetone mixture. Cryosections (5 μm) were cut with a Leica 3050 cryostat and fixed with acetone on gelatin-coated slides (Sigma). Slides were examined under an Eclipse TE300 inverted epifluorescence microscope (Nikon, Melville, NY).

To detect myofiber damage, mice were injected IP with 1% Evans blue dye (EBD; Sigma) 6 hours before they were killed. EBD is a nontoxic, hydrophilic fluorescent dye that does not penetrate biologic membranes. The principle of the assay lies in the uptake of the dye by cells with disrupted plasma membranes. The fluorescent properties of the dye allow for assessment of cell damage by fluorescence microscopy. For this assay, quadriceps muscles were excised from mice, and 5-μm cryosections were prepared for microscopic examination as described above.

Flow cytometry. Mice were killed at 7 and 10 days postinfection. Quadriceps muscles were dissected, weighed, dissociated mechanically using a syringe plunger, and incubated at 37°C for 2 hours, with vigorous shaking, in digestion buffer consisting of RPMI 1640, 10% fetal calf serum (FCS), 15 m*M* HEPES, 2.5 mg/ml of collagenase A, and 1.7 mg/ml of DNase I (all from Sigma). Cells were passed through a 70-μm cell strainer (BD Falcon, Bedford, MA) and washed 3 times in wash buffer (PBS and 15 m*M* HEPES). Cells were stained in fluorescence-activated cell sorting buffer (Hanks' balanced salt solution, 1% FCS, and 2% rabbit serum) with the fluorophore-conjugated anti-mouse antibodies NK1.1 conjugated with phycoerythrin and CD11b conjugated with fluorescein isothiocyanate (BD Biosciences, North Ryde, New South Wales, Australia). Cells were fixed overnight in 3% paraformaldehyde and analyzed on a Coulter Epics XL-MCL flow cytometer using System II software (version 3.0) (both from Coulter, Hialeah, FL).

Immunohistochemistry. For the identification of macrophages in situ, muscle was collected and fixed in paraformaldehyde/lysine/periodate (0.25% weight/volume paraformaldehyde, 0.2*M* L-lysine in sodium phosphate, and 0.43% w/v periodate) for 24 hours at 4°C. Tissues were then transferred to a 7% sucrose solution for 18–24 hours at 4°C. Fixed samples were then placed in aluminum foil and covered in Tissue-Tek OCT compound. These samples were snap-frozen in liquid nitrogen, and 7-μm sections were cut on a cryostat at −15°C. Sections were transferred to slides and stored at −20°C prior to staining.

Since decalcification interfered with the ability to detect antigens within the joint tissues, cells were prepared from total joint digests. Ankles from 3 infected mice were pooled, mechanically disrupted using a mortar and pestle, and subjected to sequential treatment with type IV collagenase (0.5 mg/ml; Sigma). The cells were adhered to glass slides by cytocentrifugation and stored at –20°C prior to staining.

Macrophages were identified in sections using F4/80 rat monoclonal antibodies and peroxidase-conjugated sheep anti-rat Ig, based on a previously published procedure (13).

Quantitative real-time polymerase chain reaction (PCR). *Organ tissue.* RNA was isolated using TRIzol (Invitrogen, Melbourne, Victoria, Australia) according to the manufacturer's instructions, after which 1 μg of RNA was reverse transcribed using an oligo(dT) primer and reverse transcriptase (Promega, Madison, WI), according to the manufacturer's instructions. A total of 100 ng of template cDNA was used for real-time PCR, which was performed on a Rotor-Gene RG-3000 instrument (Corbett Research, Sydney, New South

Wales, Australia), using QuantiTect Primer Assay kits (Qiagen, Hilden, Germany) based on quantification of the SYBR Green I fluorescent dye. The specificity of the amplification was evaluated by a melting curve analysis of the PCR products. Results were expressed as the fold change in messenger RNA (mRNA) expression, comparing infected samples with the experimental control samples (mock-inoculated and vehicle-treated). The Relative Expression Software Tool (REST; available at http://www.gene-quantification.de/rest.html) was used to calculate differences in mRNA levels, which were normalized to the housekeeping gene hypoxanthine guanine phosphoribosyltransferase.

MonoMac cells. Preparation of RNA was performed from cell pellets using an RNeasy kit, according to the manufacturer's instructions (Qiagen). Reverse transcription was conducted using random hexamers included in the TaqMan Reverse Transcription Synthesis kit (Applied Biosystems, Scoresby, Victoria, Australia), following the instructions supplied by the manufacturer. Amplification was performed in 96-well plates using an ABI Prism 7000 sequence detection system (Applied Biosystems). A human β-actin primer/probe set was used in separate wells as internal control for input cDNA.

Enzyme-linked immunosorbent assays (ELISAs) for human and mouse cytokines. The concentrations of MCP-1, MCP-2, MCP-3, macrophage inflammatory protein 1α (MIP-1α), TNFα, RANTES, and IL-8 were determined by ELISA using kits from R&D Systems (Minneapolis, MN) and Antigenix America (Huntington Station, NY), according to each manufacturer's instructions.

Nuclear extraction. Mice were inoculated as described above, killed at 7 days postinfection, and perfused for 10 minutes with PBS. Muscle tissues were collected, snap-frozen in liquid nitrogen, and ground using a mortar and pestle. For the electrophoretic mobility shift assay (EMSA), nuclear extracts were prepared according to the method described previously (28).

EMSAs. The sequences for the oligonucleotides used have been described previously (29). EMSAs were performed as reported previously (28). Briefly, oligonucleotides were labeled with ^{32}P-deoxynucleotide (Amersham, Little Chalfont, UK) using *Klenow* polymerase (Roche, Castle Hill, New South Wales, Australia). The reaction mixture contained 10 μg of nuclear extract, 5 μg of poly(dI-dC), 1 m*M* dithiothreitol, and 1 μl of ^{32}P-labeled oligonucleotides (0.1 μg/μl) dissolved in binding buffer (20 m*M* Tris HCl, 30 m*M* NaCl, 5 μ*M* EGTA, and 50% glycerol). Following incubation, electrophoresis was performed in TBE buffer (89 m*M* Tris base, 89 m*M* boric acid, and 2 m*M* EDTA) at 175V. The gels were dried and analyzed by autoradiography.

Statistical analysis. For virus titers and cytokine analyses, data were analyzed using Student's unpaired *t*-test. For disease scores, data were analyzed by Mann-Whitney U test. *P* values less than 0.05 were considered significant.

RESULTS

Specific inhibition of MCP production in vitro and in vivo by bindarit treatment. The effects of bindarit on the expression of MCPs and other proinflammatory factors were determined in a human macrophage-like cell line and in mice. MonoMac6 cells were used as a model for the production of MCPs and other proinflammatory factors following stimulation with LPS. Bindarit specifically inhibited the expression and production of MCP-1, MCP-2, and MCP-3 in these cells, while it did not affect RANTES, IL-8, or TNFα (Figures 1A–C). Similar results were also observed in RAW 264.7 cells, a murine macrophage-like cell line (data not shown).

The effects of bindarit on MCP and TNFα production were also investigated in LPS-treated mice. Consistent with what was observed in vitro, serum levels of the MCPs were significantly lower in mice treated with bindarit (Figure 1D). In addition, we performed preliminary dose-response experiments assessing the inhibition of MCP-1 production in mice with bindarit treatment. It is worth noting that the dosing regimen we used corresponded to circulating levels of bindarit that were in the range of those able to inhibit MCP-1 production in vitro (200–400 μ*M*) (data not shown).

Development of less severe disease following alphavirus infection in bindarit-treated mice. We have recently shown that MCP-1 is detected at high levels in the joint tissues of mice and humans with symptomatic infections with RRV (12). Additionally, MCP-2 and MCP-3 were also detected at high levels in the synovial joints of RRV-infected humans (data not shown). We were therefore interested to determine whether bindarit, an inhibitor of MCP synthesis (20–25) (Figure 1), could ameliorate RRV-induced disease in mice.

Mice were infected with 10^3 PFU of RRV and were given daily peritoneal injections of bindarit or a corresponding vehicle as a control. Animals were monitored daily for disease symptoms and for changes in body weight. RRV-infected mice showed disease symptoms characterized by loss of hind limb strength and hind limb dragging, and by day 8 postinfection, these mice were moribund, with a complete loss of hind limb function (Figure 2A). In contrast, RRV-infected mice receiving bindarit showed only moderate hind limb weakness (Figure 2A). RRV-infected mice failed to gain weight and, by day 10 postinfection, a mean of 3.6% loss of body mass was observed in these mice (Figure 2B). RRV-infected mice treated with bindarit showed a statistically significant increase in mean body weight from day 7 postinfection onward ($P < 0.001$ versus body mass on day 0), with mice having gained 22.2% of their mean starting body mass by day 10. Naive mock-treated mice gained ~60% of their starting weight over the same period. Despite the reduced severity of disease as a result of bindarit treatment, no significant differences

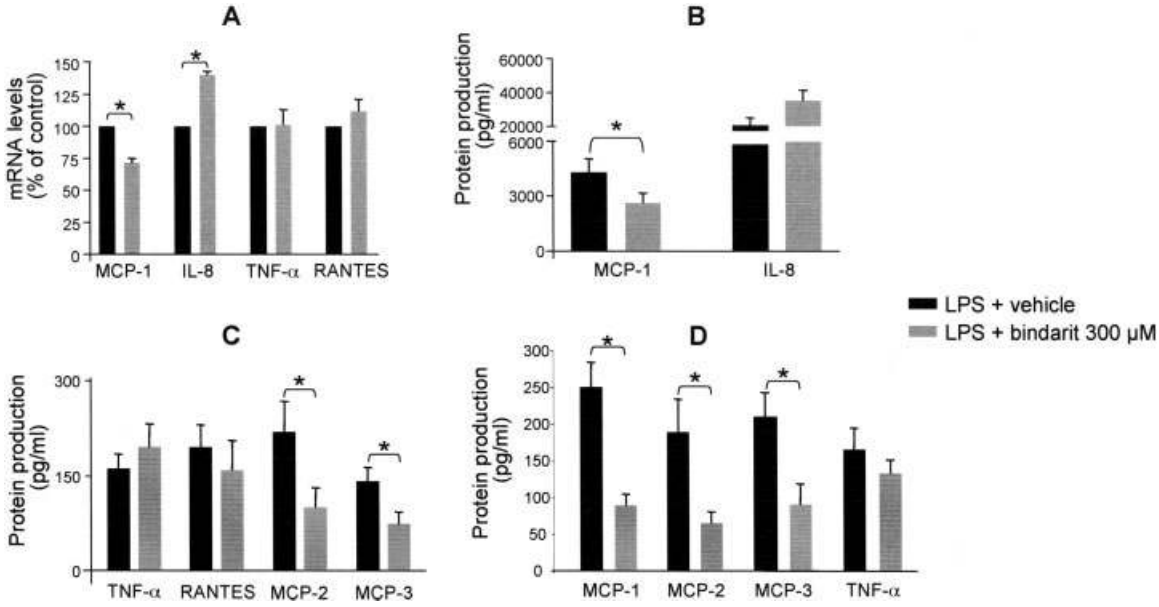

Figure 1. Effect of bindarit on the expression and production of proinflammatory factors in lipopolysaccharide (LPS)–stimulated MonoMac cells and in LPS-treated mice. Cells were preincubated for 1 hour with bindarit (300 μM) and then exposed to LPS (100 ng/ml). **A,** Total mRNA was isolated from cells following 4 hours of incubation with LPS and analyzed by quantitative real-time polymerase chain reaction for the expression of mRNA for monocyte chemotactic protein 1 (MCP-1), interleukin-8 (IL-8), tumor necrosis factor α (TNFα), and RANTES. **B** and **C,** Protein levels of MCP-1 and IL-8 (**B**) as well as TNFα, RANTES, MCP-2, and MCP-3 (**C**) were determined by enzyme-linked immunosorbent assay (ELISA) on supernatants collected after 20 hours of incubation with LPS. **D,** Mice were treated with LPS (100 μg/mouse), with or without bindarit (100 mg/kg), and serum was collected 24 hours later for ELISA determination of protein levels of MCP-1, MCP-2, MCP-3, and TNFα. Values are the mean and SD of 4 mice per group. $* = P < 0.05$ versus LPS alone, by Student's unpaired *t*-test.

were found in the RRV titers measured in the quadriceps muscles and ankle tissues from the bindarit-treated and vehicle-treated mice (Figure 2C).

We also demonstrated that bindarit treatment was more effective than anti–MCP-1 antibody treatment in ameliorating disease (Figure 3A). The therapeutic effect of bindarit was also investigated. Interestingly, bindarit was still highly effective when the start of treatment was delayed until the onset of disease symptoms (day 6) (Figure 3B).

Reduced inflammation and skeletal muscle damage following alphavirus infection in bindarit-treated mice. We have recently shown that damage to skeletal muscles in the mouse model of RRVD is mediated by inflammatory macrophages, and that these cells are a major source of MCP-1 and TNFα (12). To investigate the effects of bindarit on RRV-induced macrophage infiltration, quadriceps muscles and ankle joints were collected from mice on days 7 and 10 postinfection, and the cellular infiltrates were analyzed by histologic examination of paraffin sections, immunohistochemistry, and flow cytometry. H&E staining of tissue from RRV-infected mice showed that bindarit treatment resulted in a dramatic reduction in the total number of cells infiltrating the muscles (Figure 4C) and joints (Figure 4F), as compared with RRV-infected mice treated with vehicle alone.

We assessed the level of muscle damage in all experimental groups. Quadriceps muscles were harvested on days 7 and 10 postinfection and were weighed to assess the degree of muscle atrophy. On days 7 and 10 postinfection, the average mass of the quadriceps muscles from RRV-infected mice receiving bindarit was significantly higher than that of quadriceps muscles from controls (RRV-infected and vehicle-treated) (data not shown).

At the cellular level, damage was assessed by myofiber permeability to EBD. EBD penetrates disrupted cell membranes, and its red fluorescence allows the assessment of tissue damage via fluorescence microscopy. Uninfected mice showed little EBD penetration of muscle tissue (Figure 4G), whereas RRV-infected mice showed extensive cell membrane damage, with extensive accumulation of EBD inside myofibers (Figure 4H).

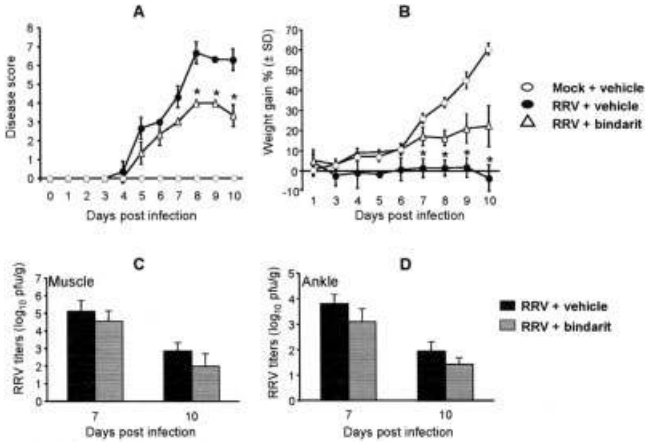

Figure 2. Effect of bindarit on Ross River virus disease (RRVD) in mice. Mice were infected subcutaneously with 10^3 plaque-forming units (PFU) of RRV. Mock-inoculated mice were injected with phosphate buffered saline alone. Mice received intraperitoneal injections of bindarit or the corresponding vehicle twice a day. **A,** Mice were scored for the development of hind limb dysfunction and disease (0–8 scale) as described in Materials and Methods. Values are the mean ± SD of 4 mice per group and are representative of 3 independent experiments. $* = P < 0.05$ versus vehicle-treated RRV-infected mice. **B,** Mice were monitored daily for changes in weight. Values are the mean ± SD of 4 mice per group. $* = P < 0.05$ versus bindarit-treated RRV-infected mice. **C** and **D,** On days 7 and 10 postinfection, the quadriceps muscles and ankle joints were collected, and the amount of virus was determined by plaque assay on Vero cells. Values are the mean and SD of 4 mice per group.

Although bindarit-treated mice showed some EBD penetration of muscle tissue, it was substantially less than that in vehicle-treated RRV-infected mice, with the dye mainly concentrated in the interstitial spaces (Figure 4I). Taken together, these results demonstrate that bindarit treatment of RRV-infected mice substantially reduced skeletal muscle damage.

Reduced macrophage infiltrates in the joint and muscle tissues of bindarit-treated RRV-infected mice. We have recently shown that the inflammatory infiltrate in this model predominantly comprises macrophages and natural killer (NK) cells (11). Using flow cytometry, the number of infiltrating cells per milligram of tissue on days 7 and 10 postinfection in the muscles of RRV-infected mice treated with bindarit was significantly lower ($P < 0.01$) than that in the muscles of RRV-infected mice treated with vehicle (Figure 5A). At 7 and 10 days postinfection, the number of CD11b+ cells per mg of tissue in the quadriceps muscles of bindarit-treated mice was 2-fold lower ($P < 0.01$) than that in the quadriceps muscles of untreated infected mice (Figure 5B), whereas the number of NK cells infiltrating the muscle was not different between bindarit-treated and vehicle-treated mice (Figure 5C). In addition, immunohistochemistry showed a similar reduction in F4/80+ cells in the joints and muscles of RRV-infected mice receiving bindarit as compared with infected mice receiving vehicle (Figure 5D). These results show that bindarit can reduce the RRV-induced infiltration of macrophages into skeletal muscle and joint tissues, and they confirm the correlation between the extent of macrophage infiltration and disease symptoms.

Reduced levels of proinflammatory mediators in bindarit-treated mice. The effect of bindarit treatment on the expression and secretion of proinflammatory mediators was assessed by real-time PCR and ELISA. As expected, mRNA and protein levels of MCP-1, MCP-2, and MCP-3 were found to be significantly lower in RRV-infected mice treated with bindarit as compared with RRV-infected animals treated with vehicle (Figures 6A–C). TNFα and type 2 nitric oxide synthase (NOS2)

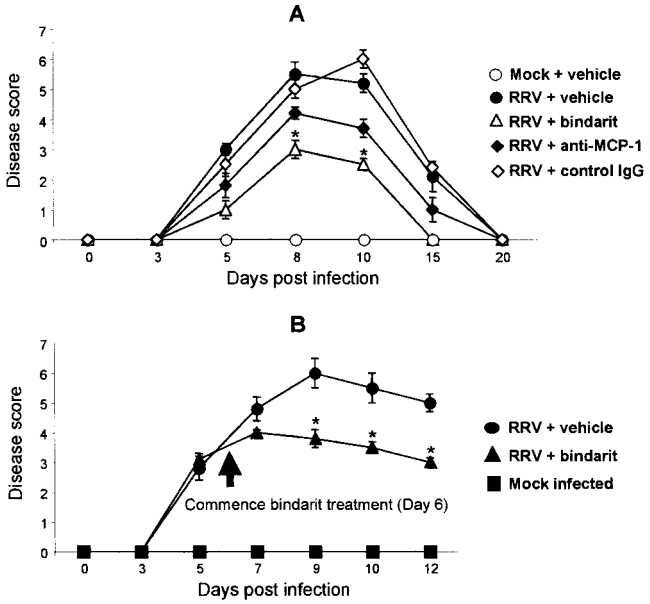

Figure 3. Effect of bindarit on Ross River virus disease (RRVD) in mice. **A,** RRV-infected mice received intraperitoneal (IP) injections of bindarit, the corresponding vehicle, anti–monocyte chemotactic protein 1 (anti–MCP-1) antibody, or control IgG. Mock-inoculated mice were injected with phosphate buffered saline alone. Mice were scored for the development of hind limb dysfunction and disease (0–8 scale) as described in Materials and Methods. Values are the mean ± SD of 4 mice per group. $* = P < 0.05$ versus anti–MCP-1–treated RRV-infected mice. **B,** RRV-infected mice were given IP injections of bindarit or the corresponding vehicle twice a day starting on day 6 postinfection (arrow). Mice were scored for the development of hind limb dysfunction and disease. Values are the mean ± SD of 4 mice per group. $* = P < 0.05$ versus vehicle-treated RRV-infected mice.

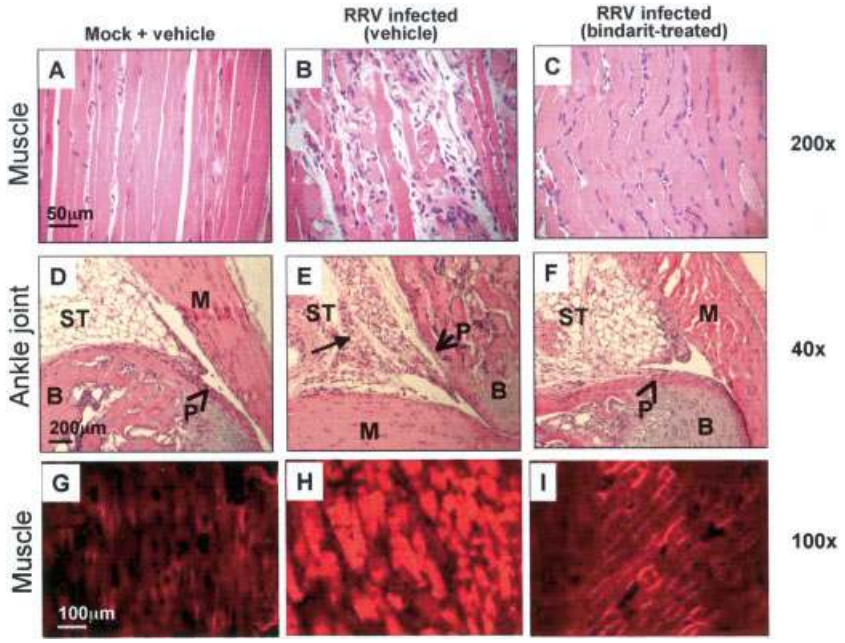

Figure 4. Effect of bindarit on Ross River virus (RRV)–induced tissue inflammation. Mice were infected subcutaneously with 10^3 plaque-forming units of RRV. Mock-inoculated mice were injected with phosphate buffered saline alone. Mice received intraperitoneal injections of bindarit or the corresponding vehicle. **A–C,** On day 7 postinfection, mice were perfused with paraformaldehyde, and the quadriceps muscles were obtained, sectioned, and stained with hematoxylin and eosin (H&E). **D–F,** On day 7 postinfection, ankle joints were obtained, decalcified, sectioned, and stained with H&E. **ST** = synovial tissue; **M** = muscle; **B** = bone; **P** = periosteum. **Arrows** indicate cell infiltration; **arrowheads** indicate periosteum. **G–I,** Mice were injected with Evans blue dye (EBD), and 6 hours later, quadriceps muscles were harvested, cryosections were prepared, and sections were examined by fluorescence microscopy for myofiber permeability to EBD. Images are representative of 4 mice per group.

levels were also reduced in RRV-infected mice receiving bindarit, perhaps as a direct consequence of the down-regulation of MCPs and the subsequent reduction in macrophage recruitment (Figures 6A–C). In contrast, the levels of MIP-1α, RANTES, IL-6, IL-1β, IFNβ, and IFNγ in both muscle and ankle tissues were not significantly different between the treatment groups (Figures 6A–C).

The effect of bindarit treatment on the activation of NF-κB in muscles was assessed by EMSA. This transcription factor is an important regulator of proinflammatory cytokine gene transcription and is known to play an important role in RA (30). NF-κB levels were significantly reduced in the muscles of RRV-infected mice receiving bindarit as compared with the muscles of RRV-infected mice receiving vehicle (Figure 6D).

DISCUSSION

RRVD and other viral arthritides are mainly treated with NSAIDs, which provide only partial relief, and new therapies are clearly needed (9). Here, we have demonstrated that bindarit treatment in a mouse model of viral arthritis reduced RRV-induced expression of MCP mRNA and protein, reduced macrophage infiltration into the muscles and joints, and consequently, reduced TNFα and NOS2 expression, resulting in reduced tissue damage and significant amelioration of disease symptoms. The mouse model of RRV mimics many of the aspects of human disease (11,12), and the results clearly indicate that inhibition of MCP synthesis with drugs such as bindarit represents a new therapeutic strategy for the treatment of RRVD and other alphaviral arthritides.

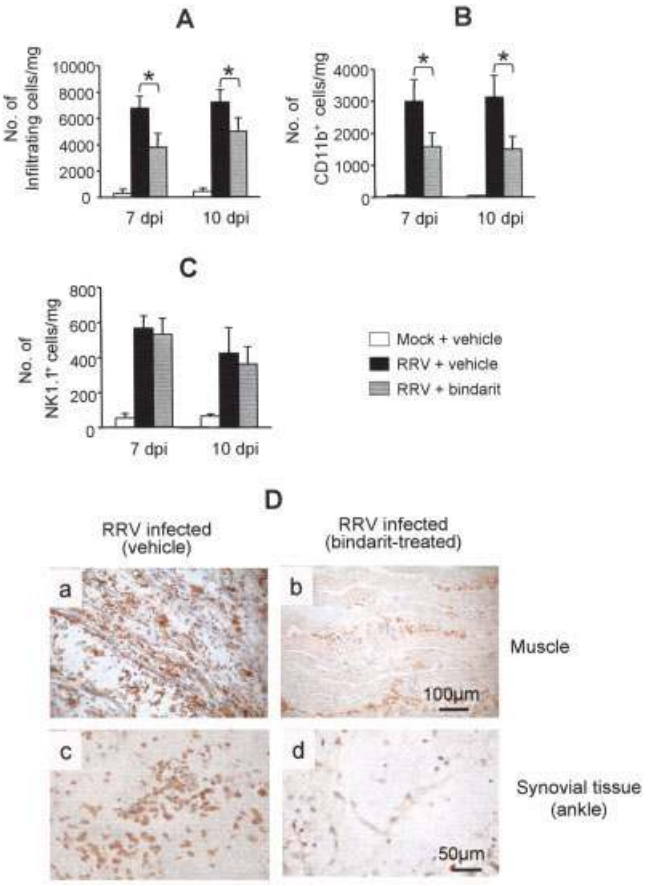

Figure 5. Effect of bindarit on Ross River virus (RRV)–induced skeletal muscle infiltration. Mice were infected subcutaneously with 10^3 plaque-forming units of RRV. Mock-inoculated mice were injected with phosphate buffered saline alone. Mice received intraperitoneal injections of bindarit or the corresponding vehicle. **A–C,** The total numbers of inflammatory cells (**A**), CD11b+ cells (**B**), and NK1.1+ cells (**C**) per milligram of tissue were determined by flow cytometry of whole quadriceps muscles on day 7 and day 10 postinfection (dpi). Values are the mean and SD of 4 mice per group. $* = P < 0.01$ by Student's unpaired *t*-test. **D,** Immunostaining for F4/80+ cells in muscle tissues (**a** and **b**) and ankle joints (cytospin) (**c** and **d**) from RRV-infected mice on day 7 postinfection. Images are representative of 4 mice per group (original magnification ×100 in **a** and **b**; ×200 in **c** and **d**).

As well as identifying inhibitors of the synthesis of MCPs as promising drug for the treatment of RRVD, the results provide additional insights into the pathogenesis of RRVD. In particular, the ability of bindarit to ameliorate disease without affecting the viral titers in the muscles and joints provides compelling evidence that the pathogenesis of RRVD is primarily an immune pathology and not directly a result of virus replication in target tissues. We speculate that this interpretation also applies to human RRVD, since steroids can ameliorate RRVD (31).

The principal role of MCP-1 is the recruitment of monocytes and macrophages, a function that has been shown to be important in a wide range of inflammatory conditions (32–34), including Lyme arthritis (35) and RRVD (1). RRV-infected synovial fibroblasts and macrophages in vitro (18) and RRV-infected muscle and joint tissues in vivo (12) express MCP-1. This is likely to be sufficient for macrophage recruitment. In RRV infection, macrophages do not appear to contribute to antiviral immunity, since their depletion had no effect on viral titers, despite a reduction in disease severity (12). The physiologic role of macrophages in this setting may be to phagocytose RRV-infected cells undergoing apoptosis, a process that is normally dominated by antiinflammatory signals (36). The production in vivo of TNFα and NOS2 suggests that the macrophages had become activated, perhaps by virus-induced IFNα/β (37) and/or T cell– or NK cell–derived IFNγ (38). It is possible that MCP-1 contributes directly to the activation of monocytes or macrophages, since a previous study demonstrated that MCP-1 induces the production of TNFα in murine peritoneal macrophages (39). TNFα and nitric oxide are well-established mediators of tissue damage and disease, and both are major products of activated macrophages (40,41). RRVD thus appears to be characterized by excessive macrophage recruitment and/or activation, with a reduction in recruitment and/or activation through suppression of the expression of MCPs that are able to significantly ameliorate disease.

In contrast to RA, relatively little is known about the spectrum of proinflammatory mediators that are produced during viral arthropathies. TNFα has been associated with human T lymphotropic virus type I arthropathy (42); IFNγ, IL-2, MCP-1, IL-6, and TNFα with caprine arthritis-encephalitis virus arthritis (43); IL-4, IL-6, IL-8, TNFα, IFNγ, MCP-1, granulocyte–macrophage colony-stimulating factor, and transforming growth factor β with parvovirus B19–associated arthritis (44); and IFNγ, TNFα, and MCP-1 with RRVD (12). From this small number of studies, the overall inflammatory mediator profile for the viral arthropathies appears to be similar to that for RA (16,40). Although therapeutic targeting of TNFα has been highly successful in the treatment of RA (40), this treatment strategy has been associated with reactivation of tuberculosis in some patients (45). Similarly, anti-TNFα therapy may need to be used with caution in viral arthritis, since this cytokine is thought to be critical for immunity to many viral infections (46). While tissue levels of TNFα were

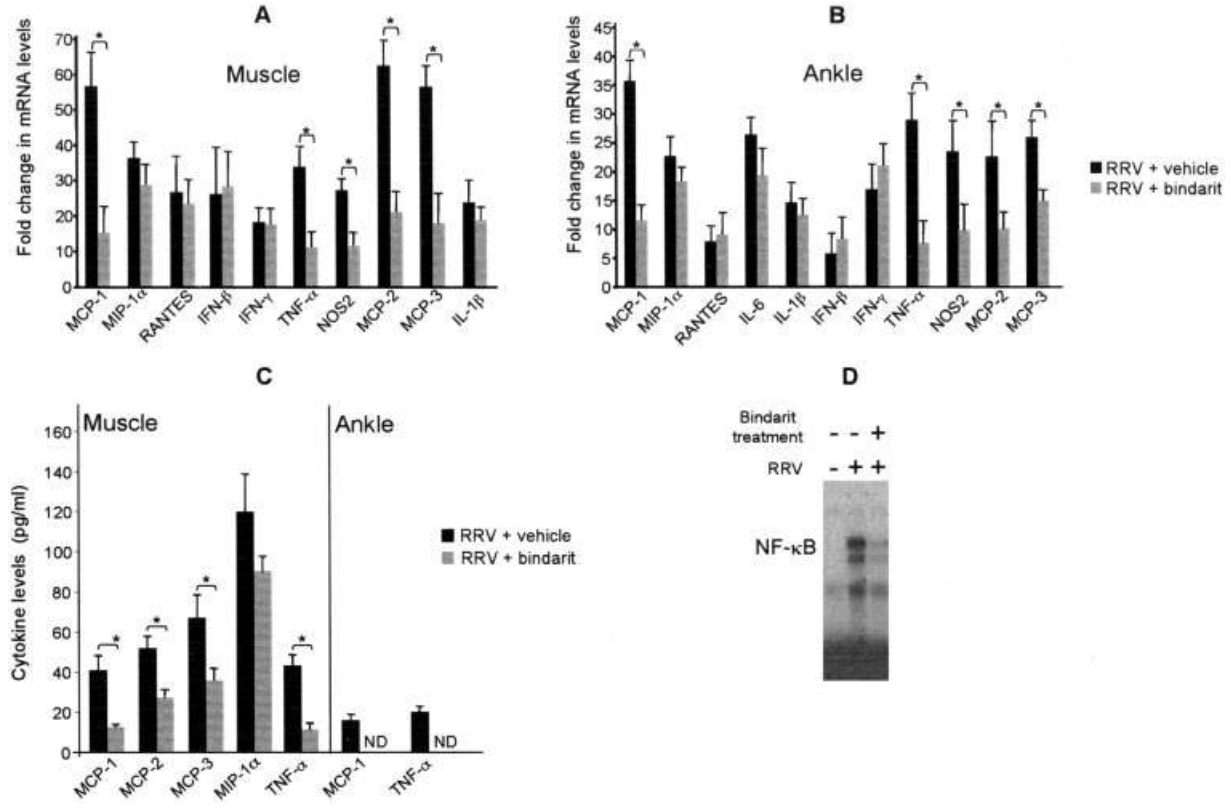

Figure 6. Effect of bindarit on the expression of proinflammatory factors in muscle and joint tissues. Mice were infected subcutaneously with 10^3 plaque-forming units of Ross River virus (RRV). Mock-inoculated mice were injected with phosphate buffered saline (PBS) alone. Mice received twice-daily intraperitoneal injections of bindarit or the corresponding vehicle beginning on the day of infection. **A** and **B,** Total mRNA was isolated from quadriceps muscles (**A**) and ankle joints (**B**) on day 7 postinfection and analyzed by real-time polymerase chain reaction for the expression of mRNA for the indicated proinflammatory factors. Values are the mean and SD fold change in mRNA levels as compared with uninfected controls (n = 4 mice per group). MIP-1α = macrophage inflammatory protein 1α; IFNβ = interferon-β; NOS2 = type 2 nitric oxide synthase (see Figure 1 for other definitions). **C,** On day 7 postinfection, mice were killed, perfused with PBS, and the quadriceps muscles and ankle joints were harvested and homogenized in PBS. Protein levels of MCP-1, MCP-2, MCP-3, MIP-1α, and TNFα in the supernatants were determined by ELISA. Values are the mean and SD of 3 mice per group. $* = P < 0.05$. ND = not detected. **D,** Activation of NF-κB in RRV-infected mice. Bindarit-treated and vehicle-treated mice were infected with RRV or were mock-inoculated. On day 7 postinfection, mice were killed, perfused for 10 minutes with PBS, and quadriceps muscles were harvested and processed for electrophoretic mobility shift assay as described in Materials and Methods.

reduced as a result of bindarit treatment (due to lower number of infiltrating macrophages), serum levels were unaffected (data not shown), suggesting that bindarit will not affect the capacity of the host to fight viral infection. MCPs are not considered to be critical mediators in the control of virus infection; hence, targeting these chemokines for the treatment of viral arthritis is unlikely to cause detrimental effects of host antiviral immunity. Importantly, as a result of the inhibition of MCPs, mice did not show signs of chronic and persistent infection (data not shown).

Bindarit is a low molecular weight entity that is capable of inhibiting the production of MCPs both in vitro and in vivo. The molecular mechanism by which this drug achieves this is currently under investigation. The efficacy and the absence of overt toxicity of bindarit in several animal models of inflammatory disease demonstrate that small-molecule inhibitors of the cytokine/chemokine system should be seriously considered as potential therapeutic agents. Moreover, a further advantage of the compound lies in its safety profile, as assessed in animals and confirmed in preliminary clinical trials in humans (26). Based on the findings of the present study, bindarit has potential as a new improved

therapy for RRVD and other viral arthritides in which macrophage infiltration may play an important immunopathologic role (42,47,48).

AUTHOR CONTRIBUTIONS

All authors were involved in drafting the article or revising it critically for important intellectual content, and all authors approved the final version to be published. Dr. Mahalingam had full access to all of the data in the study and takes responsibility for the integrity of the data and the accuracy of the data analysis.

Study conception and design. Rulli, Guglielmotti, Mangano, Mahalingam.

Acquisition of data. Rulli, Apicella, Zaid, Mahalingam.

Analysis and interpretation of data. Rulli, Rolph, Suhrbier, Mahalingam.

REFERENCES

1. Suhrbier A, La Linn M. Clinical and pathologic aspects of arthritis due to Ross River virus and other alphaviruses. Curr Opin Rheumatol 2004;16:374–9.
2. Outbreak news. Chikungunya and dengue, south-west Indian Ocean. Wkly Epidemiol Rec 2006;81:106–8.
3. Outbreak news. Chikungunya, India. Wkly Epidemiol Rec 2006; 81:409–10.
4. Rezza G, Nicoletti L, Angelini R, Romi R, Finarelli AC, Panning M, et al. CHIKV study group. Infection with chikungunya virus in Italy: an outbreak in a temperate region. Lancet 2007;370:1840–6.
5. Lanciotti RS, Ludwig ML, Rwaguma EB, Lutwama JJ, Kram TM, Karabatsos N, et al. Emergence of epidemic o'nyong-nyong fever in Uganda after a 35-year absence: genetic characterization of the virus. Virology 1998;252:258–68.
6. Harley D, Sleigh A, Ritchie S. Ross River virus transmission, infection, and disease: a cross-disciplinary review. Clin Microbiol Rev 2001;14:909–32.
7. Rulli N, Suhrbier A, Hueston L, Heise MT, Tupanceska D, Zaid A, et al. Ross River virus: molecular and cellular aspects of disease pathogenesis. Pharmacol Ther 2005;107:329–42.
8. Fraser JR. Epidemic polyarthritis and Ross River virus disease. Clin Rheum Dis 1986;12:369–88.
9. Mylonas AD, Brown AM, Carthew TL, McGrath B, Purdie DM, Pandeya N, et al. Natural history of Ross River virus-induced epidemic polyarthritis. Med J Aust 2002;177:356–60.
10. Harley D, Bossingham D, Purdie DM, Pandeya N, Sleigh AC. Ross River virus disease in tropical Queensland: evolution of rheumatic manifestations in an inception cohort followed for six months. Med J Aust 2002;77:352–5.
11. Morrison TE, Whitmore AC, Shabman RS, Lidbury BA, Mahalingam S, Heise MT. Characterization of Ross River virus tropism and virus-induced inflammation in a mouse model of viral arthritis and myositis. J Virol 2006;80:737–49.
12. Lidbury BA, Rulli NE, Suhrbier A, Smith PN, McColl SR, Cunningham AL, et al. Macrophage-derived pro-inflammatory factors contribute to the development of arthritis and myositis following infection with an arthrogenic alphavirus. J Infect Dis 2008;197:1585–93.
13. Lidbury BA, Simeonovic C, Maxwell GE, Marshall ID, Hapel AJ. Macrophage-induced muscle pathology results in morbidity and mortality for Ross River virus-infected mice. J Infect Dis 2000; 181:27–34.
14. Fraser JR, Cunningham AL, Clarris BJ, Aaskov JG, Leach R. Cytology of synovial effusions in epidemic polyarthritis. Aust N Z J Med 1981;11:168–73.
15. Szekanecz Z, Koch AE. Macrophages and their products in rheumatoid arthritis. Curr Opin Rheumatol 2007;19:289–95.
16. Asquith DL, McInnes IB. Emerging cytokine targets in rheumatoid arthritis. Curr Opin Rheumatol 2007;19:246–51.
17. Tak PP. Chemokine inhibition in inflammatory arthritis. Best Prac Res Clin Rheumatol 2006;20:929–39.
18. Mateo L, La Linn M, McColl SR, Cross S, Gardner J, Suhrbier A. An arthrogenic alphavirus induces monocyte chemoattractant protein-1 and interleukin-8. Intervirology 2000;43:55–60.
19. Guglielmotti A, D'Onofrio E, Coletta I, Aquilini L, Milanese C, Pinza M. Amelioration of rat adjuvant arthritis by therapeutic treatment with bindarit, an inhibitor of MCP-1 and TNF-α production. Inflamm Res 2002;51:252–8.
20. Guglielmotti A, Aquilini L, D'Onofrio E, Rosignoli MT, Milanese C, Pinza M. Bindarit prolongs survival and reduces renal damage in NZB/W lupus mice. Clin Exp Rheumatol 1998;16:149–54.
21. Zoja C, Corna D, Benedetti G, Morigi M, Donadelli R, Guglielmotti A, et al. Bindarit retards renal disease and prolongs survival in murine lupus autoimmune disease. Kidney Int 1998;53:726–34.
22. Bhatia M, Ramnath RD, Chevali L, Guglielmotti A. Treatment with bindarit, a blocker of MCP-1 synthesis, protects mice against acute pancreatitis. Am J Physiol Gastrointest Liver Physiol 2005; 288:1259–65.
23. Sironi M, Guglielmotti A, Polentarutti N, Fioretti F, Milanese C, Romano M, et al. A small synthetic molecule capable of preferentially inhibiting the production of the CC chemokine monocyte chemotactic protein-1. Eur Cytokine Netw 1999;10:437–42.
24. Teixeira CR, Teixeira MJ, Gomes RB, Santos CS, Andrade BB, Raffaele-Netto I, et al. Saliva from Lutzomyia longipalpis induces CC chemokine ligand 2/monocyte chemoattractant protein-1 expression and macrophage recruitment. J Immunol 2005;175: 8346–53.
25. Mirolo M, Fabbri M, Sironi M, Vecchi A, Guglielmotti A, Mangano G, et al. Impact of the anti-inflammatory agent bindarit on the chemokinome: selective inhibition of the monocyte chemotactic proteins. Eur Cytokine Netw 2008;19:119–22.
26. Perico N, Benigni A, Remuzzi G. Present and future drug treatments for chronic kidney diseases: evolving targets in renoprotection. Nat Rev Drug Discov 2008;7:936–53.
27. Kuhn RJ, Niesters HG, Hong Z, Strauss JH. Infectious RNA transcripts from Ross River virus cDNA clones and the construction and characterization of defined chimeras with Sindbis virus. Virology 1991;182:430–41.
28. Gerlag DM, Ransone L, Tak PP. The effect of a T cell-specific NF-κB inhibitor on in vitro cytokine production and collagen-induced arthritis. J Immunol 2000;165:1652–8.
29. Zare F, Bokarewa M, Nenonen N, Bergstrom T, Alexopoulou L, Flavell RA, et al. Arthritogenic properties of double-stranded (viral) RNA. J Immunol 2004;172:5656–63.
30. Tak PP, Firestein GS. NF-κB: a key role in inflammatory diseases. J Clin Invest 2001;107:7–11.
31. Mylonas AD, Harley D, Purdie DM, Pandeya N, Vecchio PC, Farmer JF, et al. Corticosteroid therapy in an alphaviral arthritis. J Clin Rheumatol 2004;10:326–30.
32. Dragomir E, Simionescu M. Monocyte chemoattractant protein-1—a major contributor to the inflammatory process associated with diabetes. Arch Physiol Biochem 2006;112:239–44.
33. Dawson J, Miltz W, Mir AK, Wiessner C. Targeting monocyte chemoattractant protein-1 signalling in disease. Expert Opin Ther Targets 2003;7:35–48.
34. Kalinowska A, Losy J. Investigational CC chemokine receptor 2 antagonists for the treatment of autoimmune diseases. Expert Opin Investig Drugs 2008;17:1267–79.
35. Brown CR, Blaho VA, Loiacono CM. Susceptibility to experimental Lyme arthritis correlates with KC and monocyte chemoattractant protein-1 production in joints and requires neutrophil recruitment via CXCR2. J Immunol 2003;171:893–901.

36. Erwig LP, Henson PM. Immunological consequences of apoptotic cell phagocytosis. Am J Pathol 2007;171:2–8.
37. Lidbury B, Mahalingam S. Specific ablation of antiviral genes in macrophages by antibody dependent enhancement of Ross River virus infection. J Virol 2000;74:8376–81.
38. Linn ML, Mateo L, Gardner J, Suhrbier A. Alphavirus-specific cytotoxic T lymphocytes recognize a cross-reactive epitope from the capsid protein and can eliminate virus from persistently infected macrophages. J Virol 1998;72:5146–53.
39. Biswas SK, Sodhi A. In vitro activation of murine peritoneal macrophages by monocyte chemoattractant protein-1: up-regulation of CD11b, production of proinflammatory cytokines, and the signal transduction pathway. J Interferon Cytokine Res 2002;22: 527–38.
40. Ackermann C, Kavanaugh A. Tumor necrosis factor as a therapeutic target of rheumatologic disease. Expert Opin Ther Targets 2007;11:1369–84.
41. Amin AR, Attur M, Abramson SB. Nitric oxide synthase and cyclooxygenases: distribution, regulation, and intervention in arthritis. Curr Opin Rheumatol 1999;11;202–9.
42. Yin W, Hasunuma T, Kobata T, Sumida T, Nishioka K. Synovial hyperplasia in HTLV-I associated arthropathy is induced by tumor necrosis factor α produced by HTLV-I infected CD68+ cells. J Rheumatol 2000;27:874–81.
43. Lechner F, Vogt HR, Seow HF, Bertoni G, Cheevers WP, von Bodungen U, et al. Expression of cytokine mRNA in lentivirus-induced arthritis. Am J Pathol 1997;151:1053–65.
44. Kerr JR, Cunniffe VS, Kelleher P, Coats AJ, Mattey DL. Circulating cytokines and chemokines in acute symptomatic parvovirus B19 infection: negative association between levels of pro-inflammatory cytokines and development of B19-associated arthritis. J Med Virol 2004;74:147–55.
45. Winthrop KL. Risk and prevention of tuberculosis and other serious opportunistic infections associated with the inhibition of tumor necrosis factor. Nat Clin Pract Rheumatol 2006;2:602–10.
46. Rahman MM, McFadden G. Modulation of tumor necrosis factor by microbial pathogens. PLoS Pathog 2006;2:e4.
47. Berger RG, Raab-Traub N. Acute monoarthritis from infectious mononucleosis. Am J Med 1999;107:177–8.
48. Wilkerson MJ, Davis WC, Baszler TV, Cheevers WP. Immunopathology of chronic lentivirus-induced arthritis. Am J Pathol 1995; 146:1433–43.